The Efficiency of Gravitational Bremsstrahlung Production in the Collision of Two Schwarzschild Black Holes

R. F. Aranha*
Centro Brasileiro de Pesquisas Físicas-CFC
Rua Dr. Xavier Sigaud 150, Urca,
Rio de Janeiro CEP 22290-180-RJ, Brazil

H. P. de Oliveira†
Instituto de Física - Universidade do Estado do Rio de Janeiro
CEP 20550-013 Rio de Janeiro, RJ, Brazil

I. Damião Soares‡
Centro Brasileiro de Pesquisas Físicas
Rua Dr. Xavier Sigaud 150, Urca,
Rio de Janeiro CEP 22290-180-RJ, Brazil

E. V. Tonini§
Centro Federal de Educação Tecnológica do Espírito Santo
Avenida Vitória, 1729, Jucutuquara, Vitória CEP 29040-780-ES, Brazil
(Dated: April 24, 2008)

We examine the efficiency of gravitational bremsstrahlung production in the process of head-on collision of two boosted Schwarzschild black holes. We constructed initial data for the characteristic initial value problem in Robinson-Trautman spacetimes, that represent two instantaneously stationary Schwarzschild black holes in motion towards each other with the same velocity. The Robinson-Trautman equation was integrated for these initial data using a numerical code based on the Galerkin method. The final resulting configuration is a boosted black hole with Bondi mass greater than the sum of the individual mass of each initial black hole. Two relevant aspects of the process are presented. The first relates the efficiency Δ of the energy extraction by gravitational wave emission to the mass of the final black hole. This relation is fitted by a distribution function of non-extensive thermostatistics with entropic parameter $q \simeq 1/2$; the result extends and validates analysis based on the linearized theory of gravitational wave emission. The second is a typical bremsstrahlung angular pattern in the early period of emission at the wave zone, a consequence of the deceleration of the black holes as they coalesce; this pattern evolves to a quadrupole form for later times.

PACS numbers:

I. INTRODUCTION

The collision of black holes, the collapse of stellar objects in the process of formation of black holes as well as the evolution of distorted black holes figure as promising sources of gravitational waves. The importance of these issues lies in the fact that the knowledge of gravitational waveforms originating from the above processes will be of crucial importance for the recent efforts to detect gravitational waves. However to date these issues still remain far from completely understood and for most situations we are forced to rely on approximation methods and numerical techniques to obtain information on wave form patterns and radiative transfer processes in the dynamics of gravitational wave emission[1].

An important astrophysical situation in which gravitational radiation is produced is that of a merger of two black

*Electronic address: rfaranha@cbpf.br
†Electronic address: oliveira@dft.if.uerj.br
‡Electronic address: ivano@cbpf.br
§Electronic address: tonini@cefetes.br

holes[2], in particular in a head-on collision, both with the same initial velocity. If the masses are distinct we should expect that the remnant of the collision would be a black hole with smaller velocity and the gravitational radiation produced to be typically bremsstrahlung in close analogy with electromagnetic bremsstrahlung.

Head-on collisions of two black holes were discussed in detail, both numerically and semi-analytically, by Aninos et al. [3], Price and Pullin[4] and Gleiser et al.[5]. The common feature of these papers is the use of Misner initial data[6] to describe the initial configuration of two equal mass nonspinning black holes. Their approach bridges numerical relativity and perturbative techniques[7] [8] to extract the gravitational wave forms at the wave zone. In Ref. [3], $l = 2$ and $l = 4$ waveforms at several radii of extraction were exhibited for one initial data set, corresponding to a proper distance between the throats for which no initial common apparent horizon is present. Also, using the extracted wave forms, the total gravitational wave energy output was calculated for six initial data sets corresponding to six distinct values of the proper distance between the throats. Initial data with small proper distance between the throats were also considered (initially close black holes) corresponding to a global initial apparent horizon. The latter situation of close black holes was examined in Ref. [4], in which the presence of a global apparent horizon allowed for the use of black hole perturbation theory; the computed gravitational radiation was in accordance with the results of numerical computations in [3]. A comparison of the different approaches in treating the head-on collision of two black holes using Misner data was given in [9]. We should also refer to Nicasio et al.[10] as a relevant reference in the problem of head-on collision of two initially boosted black holes using Brill-Lindquist type data[11]. In this vein we will consider here the interaction of two boosted black holes moving straight toward each other along the symmetry axis with the same velocity, and modeled in the context of Robinson-Trautman (RT) spacetimes[12]. In general the outcome is a boosted black hole with smaller velocity than the initial velocity of the two holes, and a larger amount of mass-energy than the sum of the individual mass-energies of the individual holes. In this process gravitational waves are emitted while the black holes decelerate and coalesce, producing a pattern typical of bremsstrahlung. RT dynamics is in the realm of characteristic initial data evolution and Bondi's mass is adopted as the total mass-energy definition.

The plan of the paper is the following. In Section 2 the basic aspects of Robinson-Trautman spacetimes are presented. Section 3 is devoted to a new construction of Brill-Lindquist type initial data for Robinson-Trautman spacetimes which can be interpreted as two initially boosted Schwarzschild black holes; the initial data adapt properly to the initial value problem on null cones as is the case in RT dynamics. The main consequences of the dynamical evolution of these initial data are discussed in Section 4, where the numerical integration is performed using a code based on the Galerkin projection method. In Section 5 we summarize our main results and discuss their relevance and limitations as compared to previous calculations of the problem in the recent literature; an outline of future perspectives in this subject is also done. Throughout the paper we use units such that $8\pi G = c = 1$.

II. ROBINSON-TRAUTMAN SPACETIMES

Robinson-Trautman (RT) metrics are solutions of vacuum Einstein's equations representing an isolated gravitational radiating system. In a suitable coordinate system they have the form

$$ds^2 = \left(\lambda(u,\theta) - \frac{2\,m_0}{r} + 2r\frac{\dot{K}}{K} \right) du^2 + 2dudr - r^2 K^2(u,\theta)(d\theta^2 + \sin^2\theta d\varphi^2). \tag{1}$$

Einstein's vacuum equations imply

$$\lambda(u,\theta) = \frac{1}{K^2} - \frac{K_{\theta\theta}}{K^3} + \frac{K_\theta^2}{K^4} - \frac{K_\theta}{K^3}\cot\theta \tag{2}$$

and

$$-6m_0\frac{\dot{K}}{K} + \frac{(\lambda_\theta \sin\theta)_\theta}{2K^2 \sin\theta} = 0. \tag{3}$$

In the above, a dot and a subscript θ denote derivatives with respect to u and θ, respectively, and m_0 corresponds to the Schwarzschild mass when $K = 1$. Throughout the paper we use units such that $8\pi G = c = 1$. The dynamics of the gravitational field is totally contained in the function $K(u,\theta)$ and governed by Eq. (3), denoted RT equation.

The initial data problem for RT spacetimes belongs to the class of characteristic initial value formulations as opposed to the 1+3 formulation, according to the classification of York[13]. The degrees of freedom of the gravitational field are contained in the conformal structure of parametrized 2-spheres embedded in a 3-spacelike hypersurface. For RT spacetimes the function $K(u_0,\theta)$ given in a characteristic surface $u = u_0$ corresponds to the initial data to be evolved via the RT equation (3).

In the semi-null local Lorentz frame given in [14] the curvature tensor of RT spacetimes is expressed as

$$R_{ABCD} = \frac{II_{ABCD}(u,\theta)}{r^3} + \frac{III_{ABCD}(u,\theta)}{r^2} + \frac{N_{ABCD}(u,\theta)}{r}, \tag{4}$$

where II, III and N are objects of Petrov-type II, III and N, respectively, displaying the peeling property[15]. Eq. 4 shows that RT indeed is the exterior gravitational field of a bounded configuration emitting gravitational waves, and for large r the spacetime looks like a gravitational wave with propagation vector $\partial/\partial r$. The curvature tensor components that contribute to the gravitational degrees of freedom transverse to the direction of propagation of the wave are

$$R_{0303} = -R_{0202} = -\frac{D(u,\theta)}{r} + \mathcal{O}\left(\frac{1}{r^2}\right), \tag{5}$$

where

$$D(u,\theta) \;=\; \frac{1}{2K^2}\partial_u\left[\frac{K_{\theta\theta}}{K} - \frac{K_\theta}{K}\cot\theta - 2\left(\frac{K_\theta}{K}\right)^2\right]. \tag{6}$$

The function D contains all the information of the angular, and time dependence of the gravitational wave amplitudes in the wave zone.

Now the basic equations (2), (3) have the stationary solution

$$K(\theta) = \frac{K_0}{\cosh\gamma \;+\; \cos\theta\;\sinh\gamma} \tag{7}$$

where K_0 and γ are constant, and as a consequence $\lambda = K_0^{-2}$ (cf. Eq. 2). According to Bondi and Sachs[16] this solution can be interpreted as a black hole boosted along the negative z-axis, with velocity parameter $v = \tanh\gamma$ and mass function $m(\theta) = m_0 K^3(\theta)$. The total mass-energy of the gravitational configuration results then in $M = m_0/2 \int_0^\pi K^3(\theta)\sin\theta d\theta = m_0\cosh\gamma = m_0/\sqrt{1-v^2}$, where for the sake of convenience we have set $K_0 = 1$. The parameter γ is associated with the rapidity parameter of a Lorentz boost given by the K-transformations of the BMS group[16]. The interpretation of (7) as a boosted black hole is relative to the asymptotic Lorentz frame which is the asymptotic rest frame of the black hole when $\gamma = 0$.

It will be important to exhibit a suitable expression for the total mass-energy content of the RT spacetimes or simply the Bondi mass. To accomplish such task it is necessary to perform a coordinate transformation to a coordinate system in which the metric coefficients satisfy the Bondi-Sachs boundary conditions (notice that in the RT coordinate system the presence of the term $2r\dot{K}/K$ does not fulfill the appropriate boundary conditions). We basically generalize the procedure outlined by Foster and Newman[17] to treat the linearized problem, whose details can be found in Ref. [18, 19]. The result of interest is that Bondi's mass function can be written for any u as $M(u,\theta) = m_0 K^3(u,\theta) +$ corrections, where the correction terms are proportional to the first and second Bondi-time derivatives of the news function; furthermore at the initial null surface $u = u_0$ these correction terms can be set to zero by properly eliminating an arbitrary function of θ appearing in the coordinate transformations from RT coordinates to Bondi's coordinates. Thus the total Bondi mass of the system at $u = u_0$ is given by

$$M(u_0) = \frac{1}{2}m_0 \int_0^\pi K^3(u_0,\theta)\,\sin\theta d\theta. \tag{8}$$

III.   BLACK HOLE INITIAL DATA FOR RT SPACETIMES

The object of this Section is to construct initial data $K(0,\theta)$ for the RT equation, representing two interacting black holes instantaneously boosted. In order to accomplish this task we will construct 3-dim initial data for two black holes (that are similar to Brill-Lindquist(BL) data[11]) from which we will extract the parametrized conformal factor $K(\theta)$ of a family of two spheres embedded in this 3-dim geometry. We will rely on the seminal paper by Misner[6] which will also be a reference for our notation in the present Section.

Starting from bispherical coordinates[20] in the 3-dim Cartesian plane Σ, we are led to introduce the following parametrization for Cartesian coordinates

$$
\begin{aligned}
x &= \frac{a \sin\theta \ \sinh\eta}{\cosh\eta - \cos\theta \ \sinh\eta} \ \cos\varphi, \\
y &= \frac{a \sin\theta \ \sinh\eta}{\cosh\eta - \cos\theta \ \sinh\eta} \ \sin\varphi, \qquad z > 0 \\
z &= \frac{a}{\cosh\eta - \cos\theta \ \sinh\eta},
\end{aligned}
\tag{9}
$$

and

$$
\begin{aligned}
x &= -\frac{a \sin\theta \ \sinh\eta}{\cosh\eta + \cos\theta \ \sinh\eta} \ \cos\varphi, \\
y &= -\frac{a \sin\theta \ \sinh\eta}{\cosh\eta + \cos\theta \ \sinh\eta} \ \sin\varphi, \qquad z < 0 \\
z &= -\frac{a}{\cosh\eta + \cos\theta \ \sinh\eta}.
\end{aligned}
\tag{10}
$$

where $0 \leq \eta \leq \infty$, $0 \leq \theta \leq \pi$, $0 \leq \varphi \leq 2\pi$. In this parametrization, for each $\eta = \eta_0$ it corresponds two spheres, one at $z > 0$ and the other at $z < 0$. Also, for a given point P of Σ in $z > 0$ fixed by $(\eta_0, \theta_0, \varphi_0)$ there is an associated unique antipodal point $P_a \to (\eta_0, \pi - \theta_0, \varphi_0)$ in the region $z < 0$, so that we go from one to the other by an inversion through the origin (cf. Fig. 1); the Cartesian vector from the origin to the point $P : (x, y, z)$ has length

$$
r_> = a\sqrt{\frac{\cosh\eta + \cos\theta \sinh\eta}{\cosh\eta - \cos\theta \sinh\eta}}
\tag{11}
$$

while its corresponding antipodal point is a distance $r_<$ from the origin given by

$$
r_< = a\sqrt{\frac{\cosh\eta - \cos\theta \sinh\eta}{\cosh\eta + \cos\theta \sinh\eta}}
\tag{12}
$$

The usefulness of this parametrization will become clear in what follows. The surface $z = 0$ corresponds to $\eta = \infty$. We note that the Cartesian coordinates are continuous functions, with continuous second derivatives, of (η, θ, φ). Singularities occurring are the usual singularities of a spherical coordinate system.

The flat space line element $ds^2 = (dx)^2 + (dy)^2 + (dz)^2$ is expressed in the above parametrization as

$$
ds^2 = a^2 \ \frac{1}{(\cosh\eta \mp \cos\theta \sinh\eta)^2} \left[d\eta^2 + \sinh^2\eta (d\theta^2 + \sin^2\theta d\varphi^2) \right]
\tag{13}
$$

for $z > 0$ and $z < 0$, respectively.

We now take Σ as a spacelike surface of initial data, with geometry defined by the line element

$$
ds^2 = K^2(\eta + \eta_0, \theta) \left[d\eta^2 + \sinh^2(\eta + \eta_0)(d\theta^2 + \sin^2\theta d\varphi^2) \right].
\tag{14}
$$

By assuming time-symmetric data (namely, Σ a maximal slice) we obtain that the Hamiltonian constraints reduce to $^{(3)}R = 0$. In this case the metric (14) must satisfy the equation

$$
\begin{aligned}
-2\frac{K_{\theta\theta}}{K^3} + \left(\frac{K'^2}{K^4} - 2\frac{K''}{K^3} - 4\frac{K'}{K^3} \coth(\eta + \eta_0) \right) \ \sinh^2(\eta + \eta_0) \\
-2\frac{K_\theta}{K^3} \cot\theta + \frac{K_\theta^2}{K^4} - 3\frac{\sinh^2(\eta + \eta_0)}{K^2} &= 0,
\end{aligned}
\tag{15}
$$

where a prime denotes derivative with respect to η. We note that the substitution $K = \Phi^2$ reduces (15) to a Laplace equation. Obviously the flat space solution

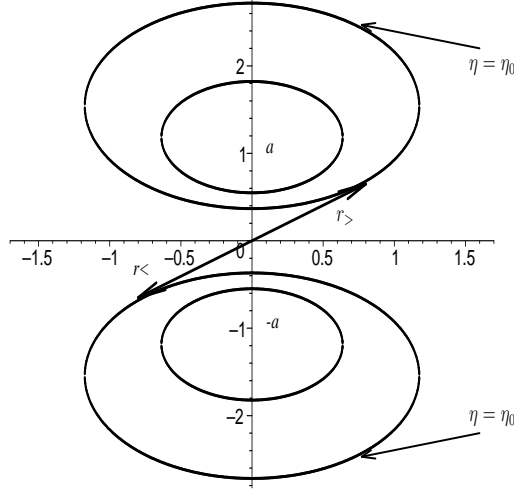FIG. 1: Projection of the spheres parametrized by η_0 into the plane xz. The Cartesian vectors $\mathbf{r}_>$ and $\mathbf{r}_<$ localize an arbitrary point of the spheres $\eta = \eta_0$ in $z > 0$ and $z < 0$, respectively.

$$K(\eta + \eta_0, \theta) = \frac{1}{\cosh(\eta + \eta_0) \mp \cos\theta \sinh(\eta + \eta_0)} \tag{16}$$

satisfies Eq. (15), from which it follows that the function

$$K(\eta, \theta) = \left(\frac{\alpha_1}{\sqrt{\cosh(\eta + \eta_0) - \cos\theta \sinh(\eta + \eta_0)}} + \frac{\alpha_2}{\sqrt{\cosh(\eta + \eta_0) + \cos\theta \sinh(\eta + \eta_0)}} \right)^2 \tag{17}$$

is a nonflat solution of (15), where α_1, α_2 and η_0 are arbitrary positive constants. We may interpret the non-flat 3-dim metric defined by (17),

$$ds^2 = a^2 \, K^2(\eta, \theta) \left[d\eta^2 + \sinh^2(\eta + \eta_0)(d\theta^2 + \sin^2\theta d\varphi^2) \right], \tag{18}$$

as a BL-type solution given in bispherical coordinates. In fact a straightforward manipulation shows that the metric (18) can be rewritten as

$$ds^2 = \frac{1}{2} \left(\alpha_2 + \alpha_1 \sqrt{\frac{\cosh(\eta + \eta_0) + \cos\theta \sinh(\eta + \eta_0)}{\cosh(\eta + \eta_0) - \cos\theta \sinh(\eta + \eta_0)}} \right)^4 ds^2_{\text{flat}(+)}$$
$$+ \frac{1}{2} \left(\alpha_1 + \alpha_2 \sqrt{\frac{\cosh(\eta + \eta_0) - \cos\theta \sinh(\eta + \eta_0)}{\cosh(\eta + \eta_0) + \cos\theta \sinh(\eta + \eta_0)}} \right)^4 ds^2_{\text{flat}(-)}, \tag{19}$$

where $ds^2_{\text{flat}(+)}$ and $ds^2_{\text{flat}(-)}$ are respectively the form of the flat space metric for the $z > 0$ and $z < 0$ domains. For $\eta \gg \eta_0$ and corresponding $x, y, z \gg a$ we may express

$$ds^2 = \frac{1}{2} \left(\alpha_2 + \frac{a\alpha_1}{r_<} \right)^4 ds^2_{\text{flat}(+)} + \frac{1}{2} \left(\alpha_1 + \frac{a\alpha_2}{r_>} \right)^4 ds^2_{\text{flat}(-)}, \tag{20}$$

and returning to Cartesian coordinates the 3-geometry can be given in the approximate form

$$g_{ij} \simeq \frac{1}{2} \left(\alpha_1{}^4 + \alpha_2{}^4 \right) \left\{ 1 + \left(\frac{4a \; \alpha_2{}^3 \alpha_1}{\alpha_1{}^4 + \alpha_2{}^4} \right) \frac{1}{r_<} + \left(\frac{4a \; \alpha_1{}^3 \alpha_2}{\alpha_1{}^4 + \alpha_2{}^4} \right) \frac{1}{r_>} \right\} \delta_{ij} \; . \tag{21}$$

This allows us to interpret the initial data (17) as two interacting Schwarzschild black holes instantaneously at rest, localized at $r_>(\eta_0)$ and $r_<(\eta_0)$, in $z > 0$ and $z < 0$, with masses $M_1 = 2\left\{ \alpha_1{}^3 \alpha_2/(\alpha_1{}^4 + \alpha_2{}^4) \right\}$ and $M_2 = 2\left\{ \alpha_2{}^3 \alpha_1/(\alpha_1{}^4 + \alpha_2{}^4) \right\}$ in units of a, respectively. It is worth noticing that the radial Schwarzschild isotropic type coordinates $r_>(\eta_0)$ and $r_>(\eta_0)$ are functions of the bispherical coordinate θ, and determine the Euclidean distance of points of the spheres $\eta = \eta_0$ to the origin. The minimal Euclidean distance between the two spheres is given by $L = (r_> + r_<)$ evaluated along the z-axis, resulting in $L = 2a \; \exp(-\eta_0)$.

From the above construction we can now extract initial data for the RT dynamics, which has its initial value problem on null cones. We note that the geometry of the two spheres located at $\eta = \eta_0$ (cf. Fig. 1) contains all the information on the initial data for vacuum field equations through the conformal function (17) calculated at $\eta = 0$. Based on the initial data formulation on characteristic surfaces proposed by D'Inverno and Stachel[21] [22], in which the degrees of freedom of the vacuum gravitational field are contained in the conformal structure of 2-spheres embedded in a 3-spacelike surface, we are then led to adopt the conformal structure given by

$$K(\eta_0, \theta) = \left(\frac{\alpha_1}{\sqrt{\cosh \eta_0 - \cos \theta \sinh \eta_0}} + \frac{\alpha_2}{\sqrt{\cosh \eta_0 + \cos \theta \sinh \eta_0}} \right)^2 \tag{22}$$

as initial data for two interacting Schwarzschild black holes to be extended along null bicharacteristics and propagated along a timelike congruence of the spacetime. A restricted spacetime of two interacting Schwarzschild black holes may then be constructed locally as the product of the two 2-sphere geometry times a timelike plane $(u, \tilde{r})$ generated by a null vector $\partial/\partial \tilde{r}$ and a timelike vector $\partial/\partial u$ with geometry $d\sigma^2 = \alpha^2(u, \tilde{r}, \theta) \; du^2 + 2 \; du \; d\tilde{r}$. The four geometry of the product space is then taken as

$$ds^2 = \alpha^2(u, \tilde{r}, \theta) \; du^2 + 2 \; du \; d\tilde{r} - \tilde{r}^2 \; K^2(\eta_0, \theta, u)(d\theta^2 + \sin^2 \theta d\varphi^2). \tag{23}$$

Eq. (23) is the Robinson-Trautman metric, the dynamics of which (ruled by Einstein's vacuum field equations) corresponds to propagating the initial data $K(\eta_0, \theta, u = 0) = K(\eta_0, \theta)$ (cf. (22)) forward in time from the characteristic initial surface $u = u_0$.

This characteristic initial data problem presents an ambiguity in the interpretation of the parameter η_0. On one hand it may be interpreted as the instantaneous boost parameter of the black holes along the z axis; on the other hand it may work as defining a distance between the two black holes. A reason for this is that the family of 2-spheres parametrized with η_0 (via the conformal factor (22)) are propagated along the timelike vector $\partial/\partial u$ that is boosted relative to the timelike vector $\partial/\partial t$. For the simple cases of $\alpha_1 = 0$ or $\alpha_2 = 0$ this boost transformation is generated by the conformal factor (22) itself[23]. We therefore are led to interpret (22) as representing two initially boosted black holes, with opposite velocities $\mathrm{v} = \tanh \eta_0$ along the z axis and with an initial Euclidean distance parameter $L/a = 2 \; \exp(-\eta_0)$.

IV. NUMERICAL RESULTS: EMISSION OF GRAVITATIONAL WAVES AND MASS LOSS

We now evolve the initial data (22) via the RT equation from $u = 0$. This equation is integrated numerically using the Galerkin method (see Refs. [14],[24] for details) in which the approximate solution of the RT equation has the following form

$$K(u, \theta) = A_0 \; \exp \left(\frac{1}{2} \sum_{k=0}^{N} b_k(u) P(\cos \theta) \right) \tag{24}$$

where A_0 is an arbitrary constant, $b_k(u)$ are unknown modal coefficients and $P_k(\cos \theta)$ are Legendre polynomials. According to the Galerkin method a set of $N+1$ ordinary differential equations determines the evolution of the modal coefficients, and therefore the function $K(u, \theta)$. The initial conditions $b_k(0)$, $k = 0, 1, .., N$ must correspond to the initial data (22) and are evaluated from

$$b_k = \frac{\left\langle 2 \ \ln \ (K(x)A_0^{-1}), P_k(\cos\theta)\right\rangle}{\left\langle P_k(\cos\theta), P_k(\cos\theta)\right\rangle}, \tag{25}$$

where the brackets define the orthogonal product in the projection space of Legendre polynomial normalized according to $\langle P_k(\cos\theta), P_j(\cos\theta)\rangle = \int_0^\pi P_k(\cos\theta), P_j(\cos\theta)\sin\theta d\theta = 2\delta_{kj}/(2k+1)$. The effect of increasing the truncation order N is illustrated in Fig. 2 with the distribution of the absolute error between the exact and approximate initial data, respectively given by (22) and $K_{\mathrm{approx}} = \exp\left(\frac{1}{2}\sum_{k=0}^N b_k(0)P(\cos\theta)\right)$.
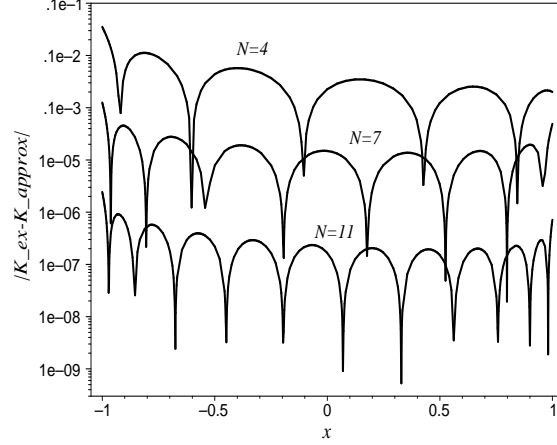

FIG. 2: Plot of the absolute error between the approximate and exact initial data for $\alpha_2 = 1.0$, $\alpha_1 = 0.2$ and $\gamma = 0.6$. The curves correspond to truncations orders $N = 4, 7, 11$. Here we have replaced the angular coordinated θ by $x = \cos\theta$.

We have done exhaustive numerical experiments considering truncation order $N = 13$ and taking into account distinct values for α_1, α_2 and η_0. Basically, the numerical outcomes can be summarized as:

- $\alpha_1 \neq \alpha_2$ (two unequal mass black holes): the final configuration is a boosted black hole with a smaller velocity, or $\eta_{0\ \mathrm{final}} < \eta_0$;

- $\alpha_1 = \alpha_2$ (two equal mass black holes): the final configuration is a black hole at rest, or $\eta_{0\ \mathrm{final}} = 0$.

The final configuration K_{final} can be reconstruct as

$$K_{\mathrm{final}}(\theta) = \exp\left(\frac{1}{2}\sum_{k=0}^N b_k(u_{\mathrm{f}})P_k(\cos\theta),\right) \tag{26}$$

where at the final time of integration $u = u_{\mathrm{f}}$, the modal coefficients $b_k(u_{\mathrm{f}}) \approx$ constant (at least up to 10^{-10}).

$$K_{\mathrm{final}}(\theta) \simeq \frac{K_{0\,\mathrm{final}}}{\cosh\eta_{0\,\mathrm{final}} + \cos\theta\ \sinh\eta_{0\,\mathrm{final}}}. \tag{27}$$

It is worth noting that for all K_{final} it is always possible to find values for $K_{0\,\mathrm{final}}$ and $\eta_{0\ \mathrm{final}}$ such as the inequality

$$|K_{\mathrm{final}}(\theta) - K_{0\,\mathrm{final}}/(\cosh\eta_{0\,\mathrm{final}} + \cos\theta\ \sinh\eta_{0\,\mathrm{final}})| \leq 10^{-7} \tag{28}$$

holds for all $0 \leq \theta \leq \pi$. Therefore the final configuration of the system is a boosted black hole; the final velocity and rest mass are determined and given respectively by $v_{\mathrm{final}} = \tanh(\eta_{0\,\mathrm{final}})$ and $m_{\mathrm{final}} = m_0 K_{0\,\mathrm{final}}^3$.

One of the most interesting aspects of the dynamics of the RT spacetimes is the emission of gravitational waves and consequently the mass loss of the initial configuration. Let us explore this feature considering the situation in

which α_2 and η_0 are fixed and α_1 is the free parameter. Therefore at $u = 0$ there are two boosted black holes directed towards each other with the same velocity and separated by a fixed distance. One of them has fixed mass while the mass of the second varies by changing α_1. In the numerical experiments we have considered the range for which $1 \ll \alpha_2/\alpha_1 \approx 1$. In particular for $\alpha_2/\alpha_1 \ll 1$ the initial data can be recast as

$$K(\theta) \simeq \frac{\alpha_2^2}{\cosh \eta_0 + \cos \theta \sinh \eta_0} + \frac{2\alpha_1 \alpha_2}{(\cosh^2 \eta_0 - \cos^2 \theta \sinh^2 \eta_0)^{1/2}}, \tag{29}$$

meaning that it can be viewed as a boosted black hole with total mass-energy $E_2 = m_0 \alpha_2^6 \cosh \eta_0$ perturbed by a smaller black hole whose total mass-energy is $E_1 = m_0 \alpha_1^6 \cosh \eta_0$ directed towards the first black hole. Noticed that since $E_1 \ll E_2$ its contribution to the total mass-energy associated to the initial data can be neglected.

According to Eq. (8) the total mass-energy of the system evaluated at $u = 0$ is given by $E_0 = 1/2 m_0 \int_0^\pi K^3(\theta) \sin \theta \, d\theta$, so that the efficiency of the process of emission of gravitational radiation can defined by[27]

$$\Delta = \frac{E_0 - M_{BH}}{E_0}, \tag{30}$$

where M_{BH} is the total mass-energy of the resulting final black hole. In the present context part of the kinetic energy and the interacting energy of both black holes is radiated away, and another part is absorbed by the first black hole increasing its rest mass to the amount $m_0 K_{0\,\text{final}}^3$. The RT equation is integrated taking into account the initial data (22) with $\eta_0 = 0.3$, $\alpha_2 = 1$ and varying α_1 inside the range $[10^{-3}, 1.3]$. For each value of α_1 the final outcome is determined and identified as a boosted black hole with smaller velocity, $v_{\text{final}} = \tanh \eta_{0\,\text{final}} < \tanh \eta_0$ and total mass-energy such that $M_{BH} > E_1 + E_2$ as expected from the area theorem of black holes[25]. In Fig. 3 the result of the numerical experiments for which $10^{-3} \leq \alpha_1 \leq 0.3$ is displayed by the plot of the efficiency Δ as function of M_{BH}, along with a continuous line accounting for an analytical function that fits quite well the numerically generated points. Then, as we have shown previously[18] the function $\Delta = \Delta(M_{BH})$ inspired from non-extensive statistics[26] is given by

$$\Delta = \Delta_{\max} (1 - y^\gamma)^{1/1-q}, \tag{31}$$

where $y = E_2/M_{BH}$ is the ratio between the initial mass-energy of the first black hole (fixed parameter α_2) and the mass-energy of the resulting black hole, $\Delta_{\max}$ is the maximum efficiency of the process attained in the limit $M_{BH} \gg E_2$; γ and q are the free parameters that characterize the non-extensive[26] relation. The best fit shown in Fig. 3 demands $\gamma \simeq 0.525$, $q \simeq 0.502$ and $\Delta_{\max} \simeq 0.000977$, which is a quite small efficiency even for a considerably high initial boost of $\tanh(0.3) \approx 0.3$ or about $90,000 \, \text{km/s}$. As a matter of fact we expect that the maximum efficiency will depend on the initial boost of both black holes. In any case the maximum efficiency is in accordance with the value about 0.07% found by Smarr and Eppley[27] for the collision of two equal and non-rotating black holes in a more general spacetime. Although the non-extensive relation (31) is in excellent agreement with the numerical results in the range of α_1 under consideration that covers the interval $M_{BH}^{\min} \leq M_{BH} \lesssim 5.0 \, M_{BH}^{\min}$, where $M_{BH}^{\min}$ is the minimum value of the mass of the final black hole, it fails to describe the entire set of points. The numerical value of the maximum efficiency, 0.000598, obtained when $\alpha_1 = \alpha_2$ is distinct from the one predicted by Eq. (31). Also for $\alpha_1 \gtrsim \alpha_2$ the efficiency seems to decrease, as would be expected from the symmetry in the interchange of α_1 and α_2 in the initial data considered.

In spite of the limitation of the non-extensive relation over entire range of numerical points, we cannot underestimate the fact expressed by the fitting of Fig. 3. Let us briefly discuss some implications of relation (31), starting from the domain of $\Delta/\Delta_{\max} \ll 1$, or relatively very small efficiency. In this situation it is clear that $E_2 \sim M_{BH}$ and therefore $y \sim 1$, so that Eq. (31) can be written as the following scaling relation

$$M_{BH} \approx E_2 \left(1 + \frac{1}{\gamma} \left(\frac{\Delta}{\Delta_{\max}} \right)^{1-q} \right). \tag{32}$$

Based on the linearized theory of gravitational wave emission we can accordingly demonstrate that the parameter q must be $1/2$, the same value obtained from our numerical experiments in the full nonlinear regime of RT dynamics. Actually, in the limit $\Delta/\Delta_{\max} \ll 1$ we might consider the initial mass given by $E_0 = E_2 + \delta E$, where $\delta E/E_2 \equiv \epsilon \ll 1$. From the quadrupole formula[28] the mass loss can be written as $\partial \delta E/\partial t \sim \mathcal{O}(\epsilon^2)$ which is negative definite. This means that the perturbation falls into the hole such that at the end its mass becomes $M_{BH} = E_2 + \delta E_{\text{abs}}$, where δE_{abs} is the total amount of mass absorbed. The other fraction of the perturbation δE_{rad} is radiated away, and as a
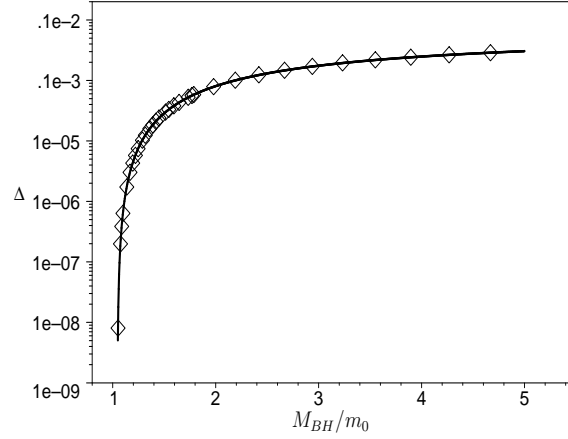
FIG. 3: Plot of the ratio M_{BH}/m_0 versus the efficiency Δ in the process of gravitational wave emission due to the collision of two black holes for $10^{-3} \leq \alpha_1 \leq 0.3$ and $\eta_0 = 0.3$. The continuous line is the best fit of the points by the function (31) with $q \simeq 1/2$.

consequence of the quadrupole formula it follows that $\delta E_{\rm rad}/E_2 \sim \mathcal{O}(\epsilon^2)$. Taking into account these relations we can express the efficiency as $\Delta = (\delta E - \delta E_{\rm abs})/E_2 \sim \mathcal{O}(\epsilon^2)$, and $1/y - 1 \sim \mathcal{O}(\epsilon)$, which leads to

$$\frac{1}{y} - 1 \propto \Delta^{1/2} \implies M_{BH} = E_2(1 + {\rm const.}\Delta^{1/2}). \tag{33}$$

Comparing Eqs. (32) and (33) we find $q = 1/2$. It must be emphasized that the above derivation is general and therefore not restricted to the realm of Robinson-Trautman spacetimes.
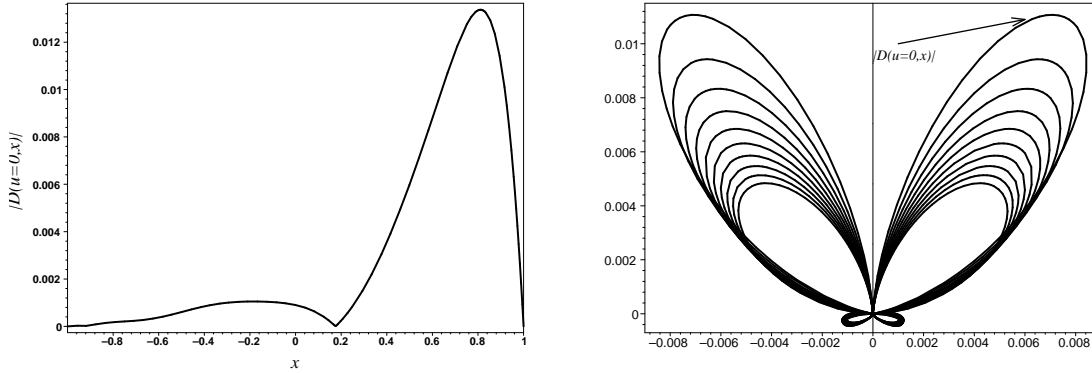

FIG. 4: Initial amplitude of gravitational waves $|D(u = 0, x)|$ for which $\alpha_1 = 0.3$, $\alpha_2 = 1$ and $\eta_0 = 0.6$. The second figure shows a sequence of polar plots of $|D(u, x)|$ at early times. Notice that the angular pattern is typical of bremsstrahlung analogous to the electromagnetic bremsstrahlung of a decelerated charge along its direction of motion, where the lobes open due to the deceleration. For later times the angular pattern evolves to a typical quadrupole form.

The second aspect we will discuss is the wave zone angular pattern of the gravitational waves emitted as described by the function $D(u, \theta)$ (cf. Eq.(6)). Its form is valid for any value of r sufficiently large since $1/r$ is a multiplicative factor to $D(u, \theta)$ in the wave zone curvature component. As we have mentioned the case $\alpha_1 = \alpha_2$ does not produce a boosted black hole due to the symmetry of the initial data. In order to illustrate the type of angular pattern of emitted waves we set $\eta_0 = 0.6$ corresponding a considerably high velocity and two black holes with initial masses of about the same order, or $\alpha_2 = 1, \alpha_1 = 0.3$. In Fig. 4(a) we show the initial pattern of these two black holes represented by the plot of $|D(u = 0, x)|$ versus $x = \cos \theta$, that exhibits a dominant emission in the northern hemisphere, with a maximum

amplitude at $x \simeq 0.81$. We note that the emission cone of maximum amplitude opens up due to the decrease in the deceleration of the system; also as it opens up the maximum amplitude decreases and the pattern evolves to a quadrupole form for later times. The final state is that of a boosted Schwarzschild black hole with $\eta_{0 \text{ final}} \approx 0.355$.

V.   CONCLUSIONS AND FINAL DISCUSSIONS

In this paper we have studied the head-on collision of two non-spinning black holes in the realm of Robinson-Trautman spacetimes. Brill-Lindquist type initial data were constructed that represent instantaneously two Schwarzschild black holes directed towards each other with the same velocity. The RT equation was integrated numerically using a combination of Galerkin and collocation methods[24] for black holes with distinct initial masses. In general the resulting configuration is a boosted black hole as described by Eq. (27) characterized by a smaller velocity than both initial velocities, while the final mass is greater than the sum of the initial masses, or $M_{BH} > E_1 + E_2$. In this process a fraction of the total initial mass is extracted by gravitational waves, whose amount has been evaluated for distinct values of the parameters.

Besides the derivation of the initial data the paper presents two relevant aspects of the dynamics in the full nonlinear regime. The first is a relation between the efficiency Δ (cf. Eq. 31) of the gravitational wave extraction and the mass of the final black hole. The remarkable feature is that the numerical results expressed by the points (M_{BH}, Δ) could be fitted by an analytical function inspired from the non-extensive statistics as we have done considering other initial data, with entropic index $q \simeq 1/2$. The question of whether or not such a relation is an artifact of Robinson-Trautman spacetimes is crucial for guiding us to further investigation on this issue. Nonetheless we have guaranteed that at least for very small efficiency the power-law (32) derived from the quadrupole formula is general (not restricted to Robinson-Trautman spacetimes) and appears as a well-defined limit of the non-extensive relation (31) with $q = 1/2$. Another important aspect we have displayed is the bremsstrahlung pattern of gravitational radiation in the wave zone, a consequence of the deceleration of both black holes as they coalesce.

As compared to previous works (Refs. [3] [4] [5] [8] [9]), most of which deals with the head-on collision of two Schwarzschild black holes, our approach differs basically in that we have adopted the characteristic surface initial data formalism. The latter indeed has several advantages for the description of the gravitational radiation and also for the construction of marching algorithms[29]. Therefore, we consider that the problem of collision of two black holes in the realm of characteristics is worth studying. In this direction, an accurate code based on the Galerkin method with collocation was constructed to integrate the field equations. The code is highly stable for long time runs in the full nonlinear regime so that we are able to reach numerically (up to 10^{-7}, cf. Eq. (28)) the final configuration of the system, when the gravitational emission ceases. The final configuration is a remnant Schwarzschild boosted black hole, with smaller velocity parameter ($\eta_{0 \text{ final}} < \eta_0$), and definite rest mass $m_{\text{final}} = m_0 K_{0 \text{ final}}^3$ and total mass-energy $M_{BH} = \left(m_0 K_{0 \text{ final}}^3 \cosh\eta_{0 \text{ final}} \right)$ (cf. Eq. (28)). We were therefore able to evaluate the efficiency of gravitational radiation emission in extracting mass-energy of the source in the full nonlinear regime as a function of the final black hole mass and the initial mass-energy of the system. This procedure is in the line of, and consistent with the general estimates made by Eardley[27]. Our approach is alternative to the one made in the above mentioned references on head-on black holes collisions, which evaluated the asymptotic energy flux carried off by the gravitational wave (or equivalently the efficiency of the gravitational wave extraction of mass from the source) through the use of the extracted gauge invariant Zerilli function[9]. The comparison of the results in the two procedures is not straightforward due to the fact that the one parameter Misner data and our three-parameter BL-type data are somewhat distinct, and numerical evaluations of the efficiency were made with variation of distinct parameters (for instance initial separation or mass-energy of the final configuration). We should mention that a few numerical tests made with fixed $\alpha_1 = 1.0$ and $\alpha_2 = 0.1$ and varying the boost parameter η_0 in our approach showed a saturation tendency of the efficiency for increasing η_0, which is in accordance qualitatively with the second order perturbation results of Ref. [10]. We expect to examine these issues in the future.

Finally, we may cite further steps in our future investigations: (i) extension of the current work by constructing and evolving initial data that represent a non-central collision of two black holes; (ii) the construction of characteristic initial data that may accommodate spinning black holes; (iii) a more general and detailed study of the amount of mass extracted by gravitational waves and (iv) the generality of the non-extensive relation (31) connecting the efficiency and the mass of the final black hole.

criticisms and suggestions that allowed to improve substantially the paper.

[1] L. Baiotti, I. Hawke, P. J. Montero, F. Loeffler, L. Rezzola, N. Stergioulas, J. A. Font and E. Seidl, *Phys. Rev. D* **71**, 024035 (2005).
[2] Frans Pretorius, *Binary Black Hole Coalescence*, preprint gr-qc/0710.1338 (2007).
[3] P. Aninos, D. Hobill, E. Seidl, L. Smarr and WM. Suen, Phys. Rev. Lett. 71, 2851 (1993).
[4] R. H. Price and J. Pullin, Phys. Rev. Lett. 72, 3297 (1994).
[5] R. J. Gleiser, C. O. Nicasio, R. H. Price and J. Pullin, Phys. Rev. Lett. 77, 4483 (1996).
[6] C. W. Misner, Phys. Rev. 118, 1110 (1960).
[7] A. M. Abrahams and C. Evans, Phys. Rev. D42, 2585 (1990).
[8] A. M. Abrahams, D. Bernstein, D. Hobill, E. Seidl and L. Smarr, Phys. Rev. D45, 3544 (1992).
[9] P. Aninos, R. H. Price, J. Pullin, E. Seidl and WM. Suen, Phys. Rev. D52, 4462 (1995).
[10] C. O. Nicasio, R. J. Gleiser, R. H. Price and J. Pullin, Phys. Rev. 59, 044024 (1999).
[11] D. R. Brill and R. W. Lindquist, Phys. Rev. 131, 471 (1963).
[12] I. Robinson and A. Trautman, *Phys. Rev. Lett.* **4**, 431 (1960); *Proc. Roy. Soc. A* **265**, 463 (1962).
[13] J.W. York Jr., *The initial value problem and dynamics*, in *G*ravitational Radiation, N. Deruelle and T. Piran, Editors, North-Holland (1983).
[14] H. P. Oliveira and I. Damião Soares, *Phys. Rev. D* **70**, 084041 (2004).
[15] A. Z. Petrov, *Sci. Nat. Kazan State University* **114**, 55 (1954); F. A. E. Pirani, *Introduction to Gravitational Radiation Theory*, in Lectures on General Relativity, Brandeis Summer Institute in Theoretical Physics, vol. 1 (Prentice-Hall, New Jersey, 1964).
[16] H. Bondi, M. G. J. van der Berg, and A. W. K. Metzner, *Proc. R. Soc. London A* **269**, 21 (1962); R. K. Sachs, *Phys. Rev.* **128**, 2851 (1962).
[17] J. Foster and E. T. Newman, J. Math. Phys. 8, 189 (1967).
[18] H. P. de Oliveira and I. Damião Soares, *Phys. Rev. D* **71**, 124034 (2005).
[19] U. Grön and D. Kramer, Class. Q. Grav. 15, 215 (1998).
[20] G. Arfken, *Mathematical Methods for Physicists*, §2.14, Academic Press (1970).
[21] R. A. D'Inverno and J. Stachel, J. Math. Phys. 19, 2447 (1978); R. A. D'Inverno and J. Smallwood, Phys. Rev. D22, 1233 (1980).
[22] J. A. Vickers in Approaches to Numerical Relativity, ed. R. d'Inverno, Cambridge University Press (Cambridge, 1992).
[23] R. K. Sachs, Phys. Rev. 128, 2851 (1962).
[24] H. P. de Oliveira, E. L. Rodrigues, I. Damião Soares and E. V. Tonini, *The low dimensional dynamical system approach in General Relativity: an example*, preprint gr-qc/0703007. To appear in the Int. J. Mod. Phys. C (2007).
[25] S. W. Hawking, Commun. Math. Phys. **25**, 152 (1972).
[26] C. Tsallis, J. Stat. Phys. 52, 479 (1988).
[27] D. Eardley, *Theoretical Models for Sources of Gravitational Waves*, in *G*ravitational Radiation, N. Deruelle and T. Piran, Editors, North-Holland (1983).
[28] C. W. Misner, K. S. Thorne and J. A. Wheeler, *Gravitation*, Freeman and Company, San Francisco (1973).
[29] Jeffrey Winicour, *Characteristic Evolution and Matching*, Living Rev. Relativity 8, (2005), 10. http://www.livingreviews.org/lrr-2005-10